Catalysis Today xxx (2016) xxx–xxx

Contents lists available at ScienceDirect

Catalysis Today

journal homepage: www.elsevier.com/locate/cattod

Bifunctional Ni catalysts for the one-pot conversion of Organosolv lignin into cycloalkanes

Xingyu Wang[a], Roberto Rinaldi[a,b,*]

[a] Max-Planck-Institut für Kohlenforschung, Kaiser-Wilhelm-Platz 1, D-45470 Mülheim an der Ruhr, Germany
[b] Department of Chemical Engineering, Imperial College London, South Kensington, Campus London, SW7 2AZ, United Kingdom

ARTICLE INFO

Article history:
Received 28 July 2015
Received in revised form
19 November 2015
Accepted 30 November 2015
Available online xxx

Keywords:
Lignin
Catalysis
Biofuels
Bifunctional catalysts

ABSTRACT

In this report, Ni/ZrO_2, Ni/Al_2O_3, Ni/Al_2O_3-KF, Ni/SBA-15, and Ni/Al-SBA-15 were examined as catalysts for the hydrodeoxygenation of diphenyl ether. Adopting the degree of deoxygenation and yield of monocyclic products as the criteria for the catalyst selection, Ni/Al-SBA-15 was identified as the best catalyst for HDO of diphenyl ether. In fact, in the presence of Ni/Al-SBA-15, full conversion of the model compound into cyclohexane was achieved with high selectivity (98%). Most strikingly, Ni/Al-SBA-15 is capable of hydrodeoxygenating Organosolv lignin with selectivity to cycloalkanes higher than 99%. Owing to the similarities to hydrocarbons derived from petroleum, the lignin-derived alkanes could well be refined into drop-in fuels by conventional oil refinery processes. Moreover, in a broader perspective, the current results also highlight the importance of Al-SBA-15, as an acidic support alternative to zeolites or other acidic materials, for the HDO of phenolic streams.

1. Introduction

Lignocellulosic biomass holds great potential as an alternative raw material for the production of liquid transportation fuels [1–4]. In fact, one of the most promising routes in today's biorefinery is the conversion of lignocellulose into fermentable sugars for the production of ethanol [5]. In this process, lignin is obtained as an unavoidable residue [6,7]. Considering current productivities of ethanol and the lignin content of lignocellulose, the production of cellulosic ethanol may release between 1 and 3 kg lignin per kg ethanol produced by fermentation of glucose [8]. Therefore, it is mandatory to find outlets for lignin utilisation. In this context, the catalytic conversion of technical lignins often generates a complex and diluted mixture of products. Hence, the isolated yield of individual products may not suffice to give a suitable return in today's chemical industry. In contrast, a lignin product mixture comprising branched aliphatics could already find uses in the fuel industry. Such a mixture could well serve both as performance-enhancer of synthetic fuels produced by the Fischer–Tropsch process and drop-in fuel in its own right [9,10].

In the current approaches for conversion of lignin into hydrocarbons, at least two steps are essential to achieving high efficiency in the hydrodeoxygenation (HDO) of lignin streams [3,4,10]. The first is the *in-situ* depolymerisation of lignin, which generates soluble lignin fragments for the catalytic conversion [4]. For some Organosolv lignins (obtained from a pulping process without added acid catalysts), a considerable quantity of relatively weak ether linkages (*e.g.,* β-O-4) may still be present in the isolated polymer. In these cases, the depolymerisation may easily take place through non-catalytic thermolysis or solvolysis at temperatures between 200 and 300 °C [11–13]. The second step consists of the catalytic conversion of (low molecular weight) fragments of lignin. Regarding the production of biofuels from lignin, the main aim of the catalyzed reactions is to remove O-functionalities selectively [10]. By reduction of ketone and aldehyde intermediates, lignin fragments are prevented from recondensation [14–17]. The prevention of recondensation is essential to mitigating problems associated with the formation of biochars, and thus improving the yield of liquid products [18–20]. Furthermore, catalytic reactions should proceed to target a reduction in O/C ratio and an increase in H/C ratio to achieve optimum fuel properties and energy density in the product [8,10]. Importantly, the cracking of the carbon backbone of lignin should target hydrocarbon products from C_9 to C_{18}, as an eventual extensive cracking of the carbon backbone decreases the energy density of the prospective fuel candidates [21].

Undoubtedly, noble metals combined with acid catalysts are promising systems for the use of lignin as feedstock for the production of biofuels *via* HDO [22]. Nonetheless, the high price of noble

* Corresponding author at: Department of Chemical Engineering, Imperial College London, South Kensington, Campus London, SW7 2AZ, United Kingdom.
E-mail address: rrinaldi@imperial.ac.uk (R. Rinaldi).

http://dx.doi.org/10.1016/j.cattod.2015.11.047
0920-5861/

metals may pose problems for such processes on a large-scale. To circumvent this limitation, the use of less expensive base metal catalysts for HDO of lignin-derived streams has been extensively explored [10,23]. In spite of the large number of reports and reviews on the upgrade of biophenols (model compounds and pyrolysis oil) available [10,24–31], to the best of our knowledge, there is no report on the use of bifunctional Ni catalysts in the HDO of Organosolv lignin rendering cycloalkanes as a distinct class of products.

In this report, aiming at improved HDO of Organosolv lignin, we first explored Ni supported on acidic or basic supports (ZrO_2, Al_2O_3, Al_2O_3/KF, SBA-15 and Al-SBA-15) for the HDO of diphenyl ether, as a model compound representing strong ether linkages (4-O-5′) in the lignin fragments. In these experiments, we identified Ni/Al-SBA–15 as the best catalyst for HDO of diphenyl ether, as it fully converts the substrate into cyclohexane with high selectivity (98%). Most strikingly, for lignin valorisation, we found that Ni/Al-SBA-15 is capable of hydrodeoxygenating Organosolv lignin, rendering cyclic alkanes at selectivity higher than 99%.

2. Experimental

2.1. Preparation of the catalytic supports

Al_2O_3-KF was prepared by suspending fumed aluminum oxide (9.0 g, Aeroxide® Alu C, Evonik) in a 0.4 mol L^{-1} KF solution (40 mL). The suspension was stirred at 70 °C for 2 h. The solid was filtered under reduced pressure and washed with distilled water at 50 °C. In sequence, the solid was dried at 120 °C under reduced pressure. The material was calcined at 450 °C for 3 h. The temperature was increased by 5 °C min^{-1} from 25 to 450 °C.

SBA-15 was prepared as described elsewhere [32]. Typically, to a solution of Pluronic P123 (4.0 g, Aldrich) dissolved in Milli-Q water (30 mL), a 2 mol L^{-1} HCl solution (120 mL) was added. In sequence, tetraethoxysilane (8.4 g, Aldrich, 99%) was added dropwise to the solution under vigorous stirring. The mixture was first aged under stirring at 38 °C for 20 h, and then statically at 100 °C for an additional 24 h. The white solid product was separated by filtration and dried in open air at room temperature. Finally, to remove the organic template, the material was calcined at 550 °C for 5 h. The temperature was increased by 5 °C min^{-1} from 25 to 550 °C.

Al-SBA-15 was prepared as described in Refs. [33–35]. Tetraethoxysilane (8.4 g), aluminum 2-propoxide (0.5 g, Aldrich, 97%) and HCl aqueous solution (10 mL, pH = 1.5) were mixed and stirred at room temperature for 3.5 h (Solution I). P123 (4 g), NH_4F (0.05 g, Aldrich, 99.99%) and HCl aqueous solution (150 mL, pH = 1.5) were mixed and stirred at 45 °C for 1 h (Solution II). Solution I was slowly added (within 10 min) to Solution II under stirring at 45 °C. The mixture was aged under stirring at 45 °C for 20 h. The solution was then transferred into a Teflon-lined autoclave, and aged under static conditions at 100 °C for 24 h. A white precipitate was formed. The white solid was collected by filtration and washed with water until pH 7. This material was dried overnight at 50 °C. Finally, the material was calcined at 550 °C for 4 h. The temperature was increased by 0.4 °C min^{-1} from 25 to 550 °C.

2.2. Catalyst preparation

Precursors of Ni/Al_2O_3, Ni/Al_2O_3-KF and Ni/ZrO_2 were prepared by incipient impregnation of Al_2O_3 (Aeroxide® Alu C, Evonik), Al_2O_3-KF, $Zr(OH)_2$ (Aldrich, 97%), respectively, with a volume of an 1.4 mol L^{-1} $Ni(NO_3)_2$ solution enough to achieve a nominal Ni loading of 10 wt%. In turn, through impregnation of SBA-15 and Al-SBA-15 with the same Ni(II) source, 5 wt% Ni/SBA-15 and Ni/Al-SBA-15 precursors were synthesised. Typically, the dried precursors were calcined at 550 °C for 5 h. The temperature was increased by 1 °C min^{-1} from 25 to 550 °C. In sequence, they were reduced under H_2/Ar (20 v/v% H_2, 250 cm^3 min^{-1}) at 550 °C for 5 h. The activated Ni catalysts were left to cool down to room temperature under H_2/Ar, and stored under argon in a glove box.

2.3. Catalyst characterisation

Transmission electron microscopy (TEM) images were taken on an HF-2000 FE transmission electron microscope at a voltage of 200 kV. Energy-dispersive X-ray spectroscopy (EDX) analysis was performed by using a Noran System Six EDX with a Si (Li) detector.

N_2 sorption analyses were carried out on an ASAP 2000 surface area analyser (Micromeritics). The specific surface was determined by using the BET method. The pore volume and pore size distribution were calculated from the desorption profiles of the isotherms by using the BJH method.

2.4. Extraction of lignin from Poplar wood through Organosolv process

Poplar wood (500 g, 2 mm chips, J. Rettenmaier & Söhne) was suspended in a 3-L solution of ethanol:water (1:1, v/v) in a 5-L reactor equipped with an overhead mechanical stirrer. The suspension was heated from 25 to 178 °C at 1.5 °C min^{-1} under mechanical stirring. The suspension was processed at 178 °C for 3.3 h. At this temperature, the autogenous pressure was 1.5 MPa. In sequence, the mixture was left to cool down to room temperature. After the wood fibers had been filtered off, a reddish–brown solution was obtained. By using a rotoevaporator, the solvent was removed under reduced pressure at 40 °C. A solid reddish–brown residue (116 g, Organosolv lignin) was obtained. Elemental analysis: C, 59.0%; H, 6.2%; N, 0.1%, O, 34.7%. GPC characterisation (values given by comparison with PS standards in THF): M_w 960 Da; M_n 330 Da.

2.5. Catalytic experiments

2.5.1. Hydrodeoxygenation of diphenyl ether

All the procedures involving the activated catalysts were performed in a glove–box under Argon. In a glass inlet, a catalyst (100 mg) was suspended in a solution containing diphenyl ether (500 mg, Aldrich, 99.9%), *n*-dibutyl ether (100 mg, internal standard, Aldrich, 99.3%) and solvent (15 mL, methylcyclohexane, Aldrich 99.9%). The glass inlet was then placed into a stainless steel reactor (30 mL). After removing the autoclave from the glove–box, the reactor vessel was flushed with H_2 and then loaded with an H_2 pressure of 5 MPa (measured at 25 °C). The experiments were performed under overhead mechanical stirring (400 rpm) at 200 °C for 40 min. The reaction medium was analysed by GC–FID and GC–MS.

2.5.2. Hydrodeoxygenation of Organosolv lignin

In a glass inlet, Organosolv lignin (500 mg) and Ni/Al-SBA-15 (150 mg) were suspended in methylcyclohexane (15 mL) under argon (glove–box). The glass inlet was then placed into a stainless steel reactor (30 mL). After removing the autoclave from the glove–box, the reactor vessel was flushed with H_2 and then loaded with an initial H_2 pressure of 7 MPa (measured at 25 °C). The experiments were performed under overhead mechanical stirring (400–rpm) at 300 °C for 8 h. After the reaction, *n*-dibutyl ether was added to the reaction mixture (external standard for the GC × GC–FID analysis). The reaction mixture was filtered. The solid residue (containing the catalyst and lignin residues) was washed with methylcyclohexane, dried at 60 °C under vacuum, and then weighed. The consumption of lignin was determined by weight difference.

Please cite this article in press as: X. Wang, R. Rinaldi, Bifunctional Ni catalysts for the one-pot conversion of Organosolv lignin into cycloalkanes, Catal. Today (2016), http://dx.doi.org/10.1016/j.cattod.2015.11.047

2.6. Quantification of the products

2.6.1. GC analysis

The samples were analysed on a gas chromatograph (Shimadzu QP2010 Plus) equipped with a Rxi-1 ms column (30 m). The temperature program started with an isothermal step at 40 °C for 6 min. Next, the temperature was increased by 30 °C min^{-1} to another isothermal step at 160 °C for 1 min. Again, the temperature was raised to 200 °C by 30 °C min^{-1}. From this point on, the temperature was increased at 10 °C min^{-1} up to the last isothermal step at 240 °C for 1 min. The components were identified by using mass spectra (MS) libraries NIST 08, NIST 08s and Wiley 9. The quantification was performed using the calibration curves based on the response of the flame ionisation detector (FID) for each component of the mixture.

2.6.2. GC × GC Analysis

The reaction mixtures were analysed by using 2D GC × GC–MS (1st column: Rxi-1 ms 30 m, 0.25 mm ID, d_f 0.25 μm; 2nd column: BPX50, 1 m, 0.15 mm ID, d_f 0.15 μm) in a gas chromatograph (Shimadzu QP2010 Plus) equipped with a ZX1 thermal modulation system (Zoex). The temperature program started with an isothermal step at 40 °C for 5 min. Next, the temperature was increased from 30 °C to 300 °C by 5.2 °C min^{-1}. The program finished with an isothermal step at 300 °C for 5 min. The modulation applied to the comprehensive GC × GC analysis was a hot-jet pulse (400 ms) every 9000 ms. 2D chromatograms were processed by using GC Image software (Zoex). The products were identified by using MS libraries NIST 08, NIST 08s, and Wiley 9. The semiquantification of the products was performed using the GC × GC–FID images and estimated response factors.

3. Results and discussion

3.1. Characterisation of the supported Ni catalysts

Shown in Fig. 1 are TEM images of 10 wt% Ni/ZrO_2, Ni/Al_2O_3 and Ni/Al_2O_3-KF catalysts. Clearly, the supports consist of packed particles. The particle packing generates a non-structural pore system in the materials. Moreover, the metal nanoparticles can be distinguished (dark spots) from the support. The average size of Ni particles depends on the carriers. Ni particles on ZnO_2 and Al_2O_3 were formed with an average size of 5–10 nm, while on Al_2O_3-KF with 10–20 nm.

Displayed in Fig. 2 are TEM images of 5 wt% Ni/SBA-15 and Ni/Al-SBA-15. For both materials, the highly ordered hexagonal mesostructure was preserved throughout the procedure of catalyst preparation. Small Ni particles (~6 nm) are detected inside the channels (Fig. 2b and d), but a significant amount of large Ni particles (30–50 nm) are located on the external support surface (Fig. 2a–c). The presence of Ni particles on the outer surface of Al-SBA-15 most likely constitutes an advantageous feature for the hydrogenolysis and hydrogenation of large fragments of lignin, which could face problems to access the internal surface of Al-SBA-15 for catalytic conversion, accounting for the outstanding results obtained from the HDO of lignin using this material as a catalyst (*vide infra*).

Listed in Table 1 are the textural properties of Ni catalysts as determined by N_2 physisorption. As expected, Ni/ZrO_2, Ni/Al_2O_3 and Ni/Al_2O_3-KF have low BET surface area (76–110 m^2 g^{-1}) and pore volume (0.2–0.5 cm^3 g^{-1}). The loading of Ni slightly decreased the surface area of Al_2O_3 (from 110 to 99 m^2 g^{-1}), but considerably increased the pore volume (from 0.19 to 0.45 cm^3 g^{-1}, entries 1 and 2). It is clear that the incipient impregnation led to aggregation of individual Al_2O_3 particles, which reduces the surface area,

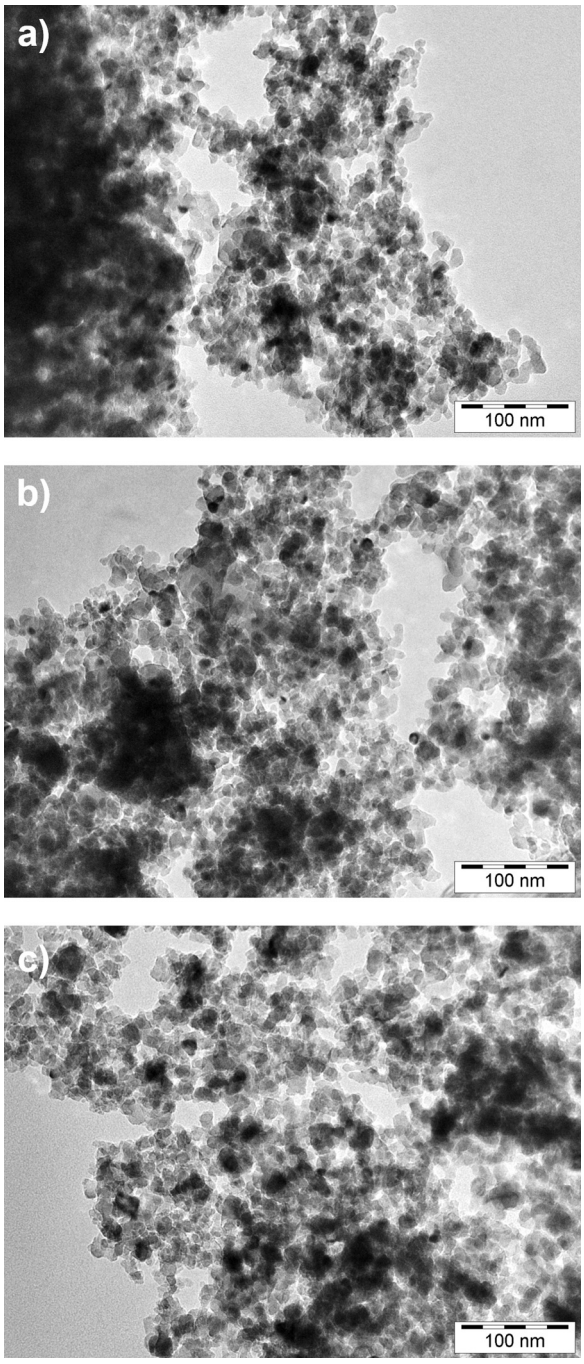

Fig. 1. TEM images of (a) Ni/ZrO_2, (b) Ni/Al_2O_3, (c) Ni/Al_2O_3-KF.

Table 1
Textural properties of supports and Ni catalysts.

Entry	Material	BET surface (m^2 g^{-1})	Pore volume (cm^3 g^{-1})	Average pore size (nm)
1	Ni/ZrO_2	77	0.20	11.3
2	Al_2O_3	110	0.19	11.6
3	Ni/Al_2O_3	99	0.45	27.1
4	Ni/Al_2O_3-KF	99	0.47	33.4
5	SBA-15	837	1.23	7.2
6	Al-SBA-15	821	1.32	8.2
7	Ni/SBA-15	645	0.90	6.7
8	Ni/Al-SBA-15	607	0.93	7.7

Please cite this article in press as: X. Wang, R. Rinaldi, Bifunctional Ni catalysts for the one-pot conversion of Organosolv lignin into cycloalkanes, Catal. Today (2016), http://dx.doi.org/10.1016/j.cattod.2015.11.047

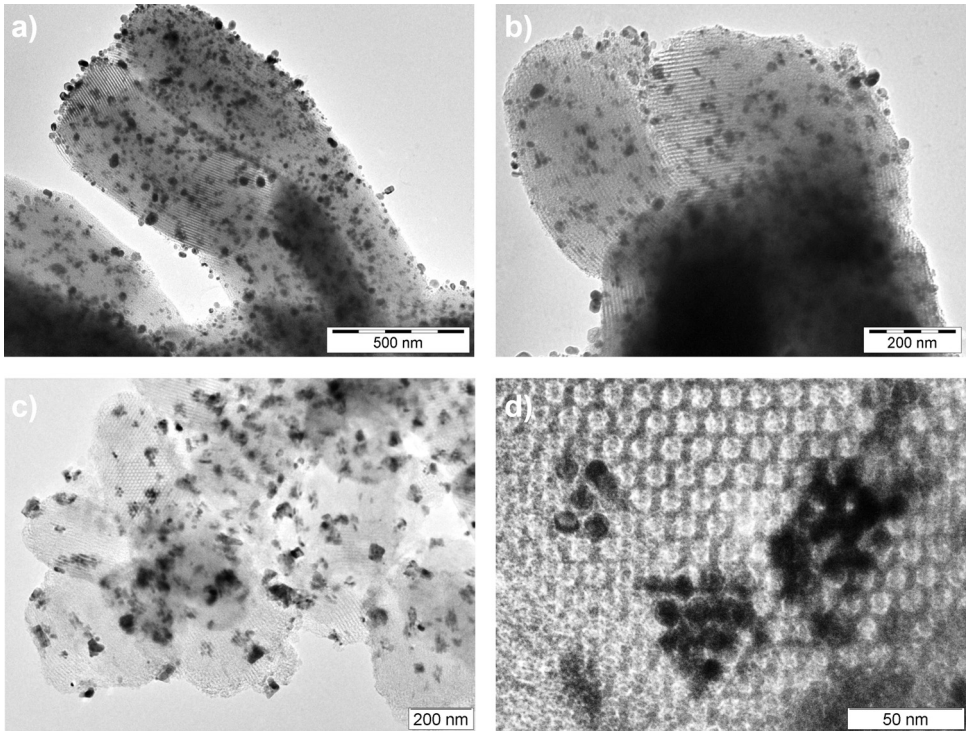

Fig. 2. TEM images of Ni catalysts supported on a, b): SBA-15 and c, d): Al-SBA-15.

but creates a pore structure, and therefore, increases the pore volume. KF treatment did not significantly affect the pore structure of Ni/Al_2O_3-KF, as revealed by the similar textural properties found for Ni/Al_2O_3 and Ni/Al_2O_3-KF (Table 1, entries 3 and 4). In turn, SBA-15 and Al-SBA-15 show high surface area (> 800 $m^2\,g^{-1}$) and high pore volume (> 1.2 $cm^3\,g^{-1}$) with an average pore size between 7 and 8 nm. As expected, the loading of Ni decreased the surface area, pore volume, and average pore size (Table 1, entries 5–8). The drop in surface area is another evidence of a partial deposition of Ni particles inside the channels of SBA-15 and Al-SBA-15, as also seen in TEM images of these materials (Fig. 2).

To gain more detail on the pore structure of the materials, N_2 adsorption–desorption isotherms were examined (Fig. 3 and Fig. 4). N_2 adsorption and desorption profile found for Ni/ZrO_2 shows a type IV isotherm with H1 + H3 hysteresis loops (Fig. 3a), which characterise a mesoporous structure with undefined pore shape [36,37]. Again, the sharp step at P/P_0 range of 0.9–1.0 suggests a contribution of non-structural pores formed by particle packing. Furthermore, isotherms of type II were observed for Al_2O_3, Ni/Al_2O_3 and Ni/Al_2O_3-KF (Fig. 3b–d), indicating that these materials are non-porous solids. Again, type H3 hysteresis loop indicates the presence of non-structural mesopores formed by particle packing [38].

N_2 adsorption–desorption isotherms found for SBA-15 and Al-SBA-15 is of type IV with an H1 hysteresis loop (Fig. 4a and b), which describes a mesoporous material with cylindrical pores with a narrow size distribution [39]. For Ni/SBA-15 and Ni/Al-SBA-15, a second step in isotherms is detected at $P/P_0 \sim 0.8$ (Fig. 4c and d). The stepwise adsorption isotherm (Type IV) observed for Ni/SBA-15 and Ni/Al-SBA-15 indicates the presence of a multi-model pore distribution, which is expected from the non-uniform loading of the pore system by Ni nanoparticles, as shown by TEM images (Fig. 4). Despite this, the mesoporous structure was preserved after the loading of the Ni phase, as shown by HR-TEM (Fig. 2).

3.2. Catalytic conversion of diphenyl ether

Hydrogenolysis of diphenyl ether was investigated as a model reaction for the upgrade of lignin. He et al.]40–42] demonstrated that the product distribution obtained from the Ni-catalyzed conversion of diphenyl ether is determined by two parallel reaction channels, namely, hydrogenation of aromatic ring and hydrogenolysis of C—O ether bond (Scheme 1) [40–42]. Notably, upon the stepwise saturation of diphenyl ether (*i.e.* **1** → **2** → **3**), the reactivity of the ether bond toward hydrogenolysis dramatically decreases. In fact, monofunctional Ni catalysts are inactive for the hydrogenolysis of Csp^3—O—Csp^3 linkages [4,40–42]. Accordingly, the full saturation of diphenyl ether leads to a dead end in the HDO process if no acidic functionality is present in the catalyst [4]. However, provided that acid sites of adequate strength are present on the catalyst surface, the dialkyl ether intermediate may then undergo hydrolysis, consuming the water formed by the dehydration of cyclohexanol intermediate through other reaction channels. As a result, cyclohexane is obtained from the reaction channel: cyclohexanol → cyclohexene → cyclohexane, as represented in Scheme 1.

To examine the catalytic performance of the supported Ni materials, the reactions were carried out in methylcyclohexane (solvent) under 5 MPa H_2 (*r.t.*) at 200 °C for 40 min. Summarised in Table 2 are the results of the catalytic conversion of diphenyl ether, selectivity to products, and the ratio of monocyclic products to bicyclic products [Σ(4–7)/Σ(2,3)] in addition to the ratio of oxygenated monocyclic products to deoxygenated monocyclic products [Σ(4,6)/Σ(5,7)].

In the presence of Raney Ni, Ni/SBA-15 or Ni/Al-SBA-15, full conversion of diphenyl ether was achieved after 40 min (entries 1, 5 and 6). From these experiments, only saturated products were obtained. However, with Ni/ZrO_2, Ni/Al_2O_3 or Ni/Al_2O_3-KF, high conversion (96–99%) was achieved, but unsaturated compounds

Please cite this article in press as: X. Wang, R. Rinaldi, Bifunctional Ni catalysts for the one-pot conversion of Organosolv lignin into cycloalkanes, Catal. Today (2016), http://dx.doi.org/10.1016/j.cattod.2015.11.047

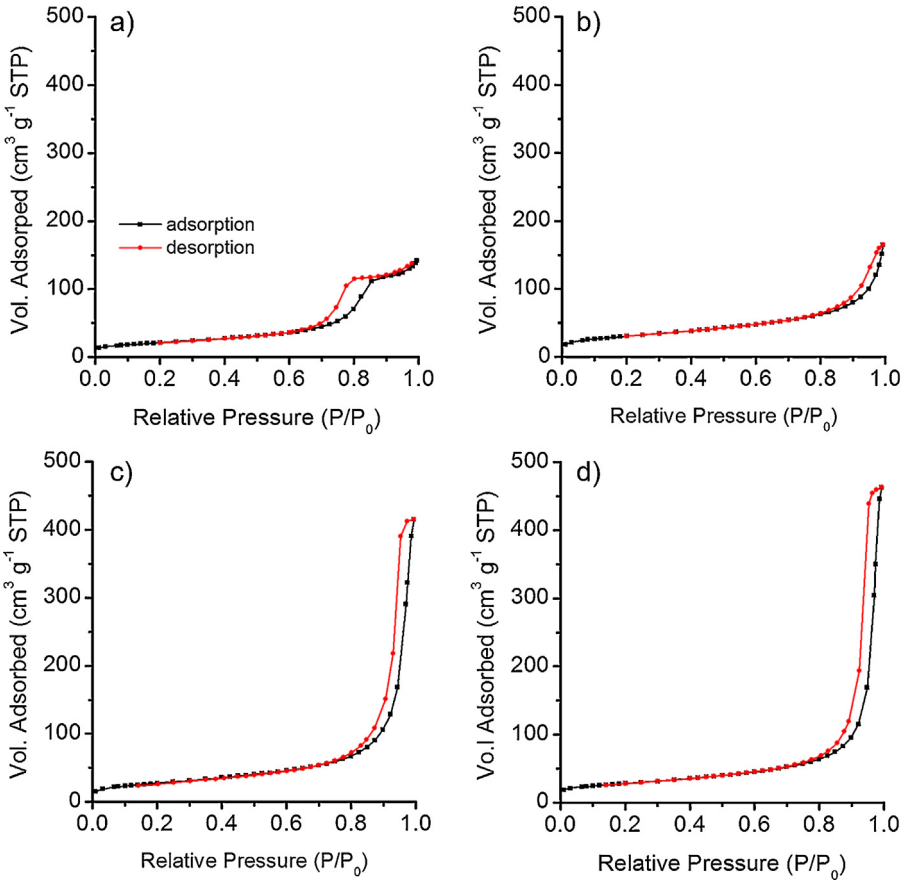

Fig. 3. Nitrogen adsorption–desorption isotherms of (a) Ni/ZrO_2, (b) Al_2O_3, (c) Ni/Al_2O_3 and (d) Ni/Al_2O_3-KF.

Table 2
Results of the conversion of diphenyl ether in the presence of a benchmark catalyst (Raney Ni) and supported Ni catalysts.

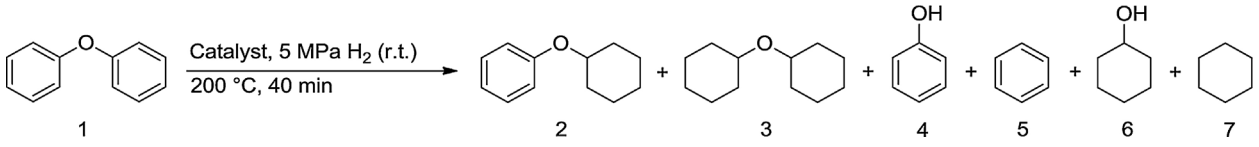

1 2 3 4 5 6 7

Entry	Catalyst	Conv. (%)	Selectivity (%)						Σ(4–7) / Σ(2,3)	Σ(4,6) / Σ(5,7)
			2	3	4	5	6	7		
1	Raney Ni	100	0	38	0	0	29	32	1.6	0.91
2	Ni/ZrO_2	96	14	19	0	8	24	32	1.9	0.61
3	Ni/Al_2O_3	99	3	44	0	0	24	29	1.2	0.85
4	Ni/Al_2O_3-KF	99	2	35	0	0	32	31	1.7	1.01
5	Ni/SBA-15	100	0	50	0	0	23	27	1.0	0.87
6[b]	Ni/Al-SBA-15	100	0	0	0	0	0	98	98/0	0.00

[a] Reaction conditions: diphenyl ether (2.9 mmol), dibutyl ether (internal standard, 0.78 mmol), catalyst (100 mg) and solvent (15 mL), 5 MPa (r.t.), 200 °C for 40 min.
[b] 1,1′-bicyclohexane was obtained as a minor product (2%).

were still detected (entries 2–4). To compare the selectivity values, the ratios [Σ(4–7)/Σ(2,3)] and [Σ(4,6)/Σ(5,7)] were analysed. On the one hand, the ratio Σ(4–7)/Σ(2,3) describes the selectivity to monocyclic products produced by the cleavage of C—O bond. On the other hand, the ratio Σ(4,6)/Σ(5,7) defines the selectivity to hydrodeoxygenation after the ether bond cleavage, that is, the ability of the catalyst to perform the reaction sequence: phenol → cyclohexanol → cyclohexene → cyclohexane [4,20].

In Table 2, entries 1–5 indicate that the Σ(4–7)/Σ(2,3) ratio obtained from experiments with Ni/Al_2O_3 (1.2) and Ni/SBA-15 (1.0) is lower than that found for the experiment with Raney Ni (1.6). However, with Ni/ZrO_2 (1.9) and Ni/Al_2O_3-KF(1.7) the ratio is slightly higher than with Raney Ni (1.6). Remarkably, subjecting diphenyl ether to Ni/Al-SBA-15 renders a 98% yield of cyclohexane. Overall, the selectivity to monocyclic products increases as follows Ni/SBA-15 < Ni/Al_2O_3 < Raney Ni < Ni/Al_2O_3-KF < Ni/ZrO_2 «< Ni/Al-SBA-15.

Regarding the degree of hydrodeoxygenation, the ratio Σ(4,6)/Σ(5,7) obtained from experiments with Ni/ZrO_2 (0.61), Ni/Al_2O_3 (0.85), Ni/SBA-15 (0.87) and Raney Ni (0.91) indicate that hydrodeoxygenation is achieved to only a very limited extent. In turn, Ni/Al_2O_3-KF shows no deoxygenation activity (Σ(4,6)/Σ(5,7) = 1.0). Obviously, the support acidity is of great significance in the deoxygenation. ZrO_2 and Al_2O_3 both contain acidic

Please cite this article in press as: X. Wang, R. Rinaldi, Bifunctional Ni catalysts for the one-pot conversion of Organosolv lignin into cycloalkanes, Catal. Today (2016), http://dx.doi.org/10.1016/j.cattod.2015.11.047

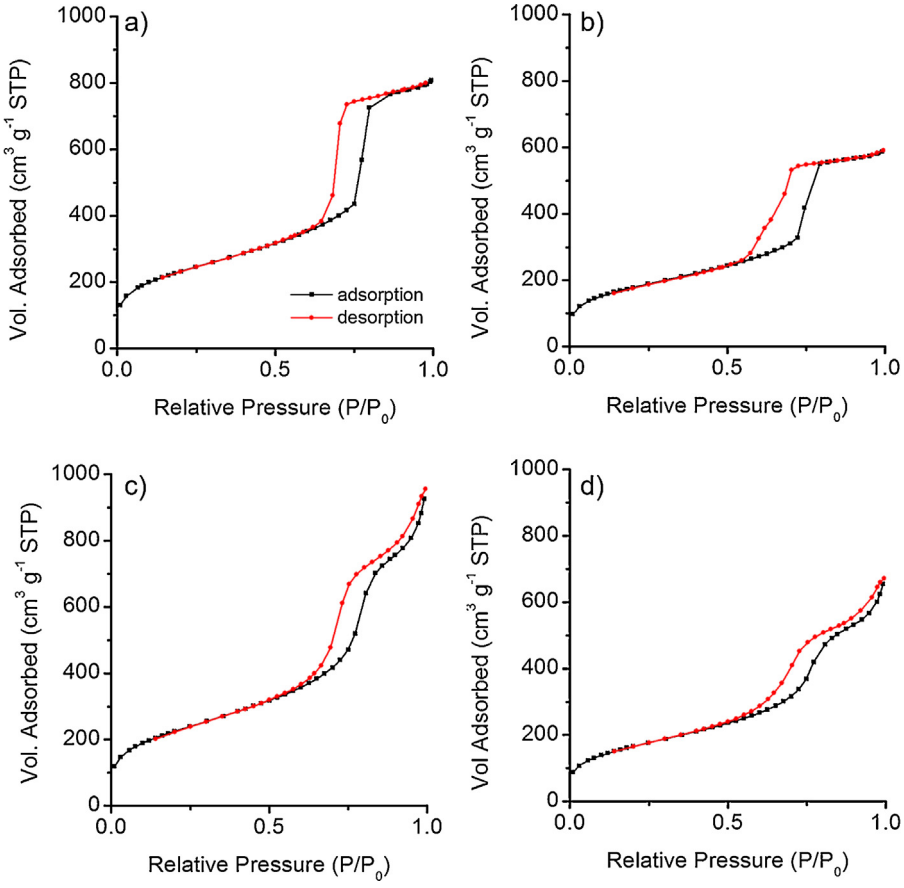

Fig. 4. Nitrogen adsorption–desorption isotherms of (a) SBA-15, (b) Al-SBA-15, (c) Ni/SBA-15 and (d) Ni/Al-SBA-15.

sites of moderate acid strength [43]. which can catalyze the deoxygenation *via* dehydration of cyclic alcohol [44,45]. More important, however, are the results obtained from the experiment in the presence of Ni/Al-SBA-15. In this case, the hydrogenolysis of diphenyl ether proceeded to full conversion yielding cyclohexane (98%) and 1,1′-bicyclohexane (2%) (Table 2, Entry 6). Conversely, the reaction in the presence of Ni/SBA-15 rendered dicyclohexyl ether (50%), cyclohexanol (23%) and cyclohexane (27%). Clearly, the absence of strong acid sites in SBA-15 causes the accumulation of dicyclohexyl ether and cyclohexanol in the product mixture. These results confirm that the hydrogenation ability of Ni phase together with high surface area (607 m^2 g^{-1}) of the highly acidic support (Al-SBA-15) [35] hold the key to providing a highly active material for the conversion of diphenyl ether into cyclohexane.

3.3. Conversion of Organosolv lignin

To assess the performance of Ni/Al-SBA-15 in the conversion of Organosolv lignin the substrate was subjected to Ni/Al-SBA-15 suspended in methylcyclohexane under an H_2 pressure of 7.0 MPa

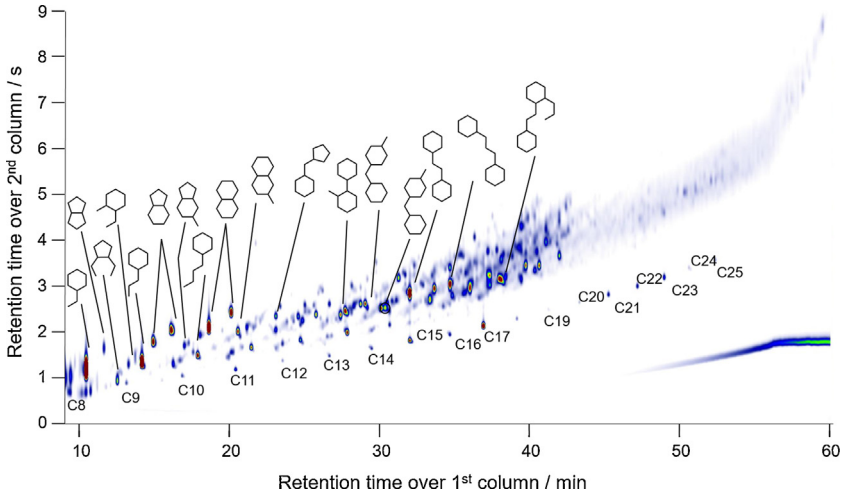

Fig. 5. GC × GC image of the products obtained from the HDO of organosolv lignin. Reaction conditions: reaction conditions: Organosolv lignin (0.5 g), methylcyclohexane (15 mL), Ni/Al-SBA-15 (200 mg), 7 MPa H_2 (r.t.), 8 h.

Please cite this article in press as: X. Wang, R. Rinaldi, Bifunctional Ni catalysts for the one-pot conversion of Organosolv lignin into cycloalkanes, Catal. Today (2016), http://dx.doi.org/10.1016/j.cattod.2015.11.047

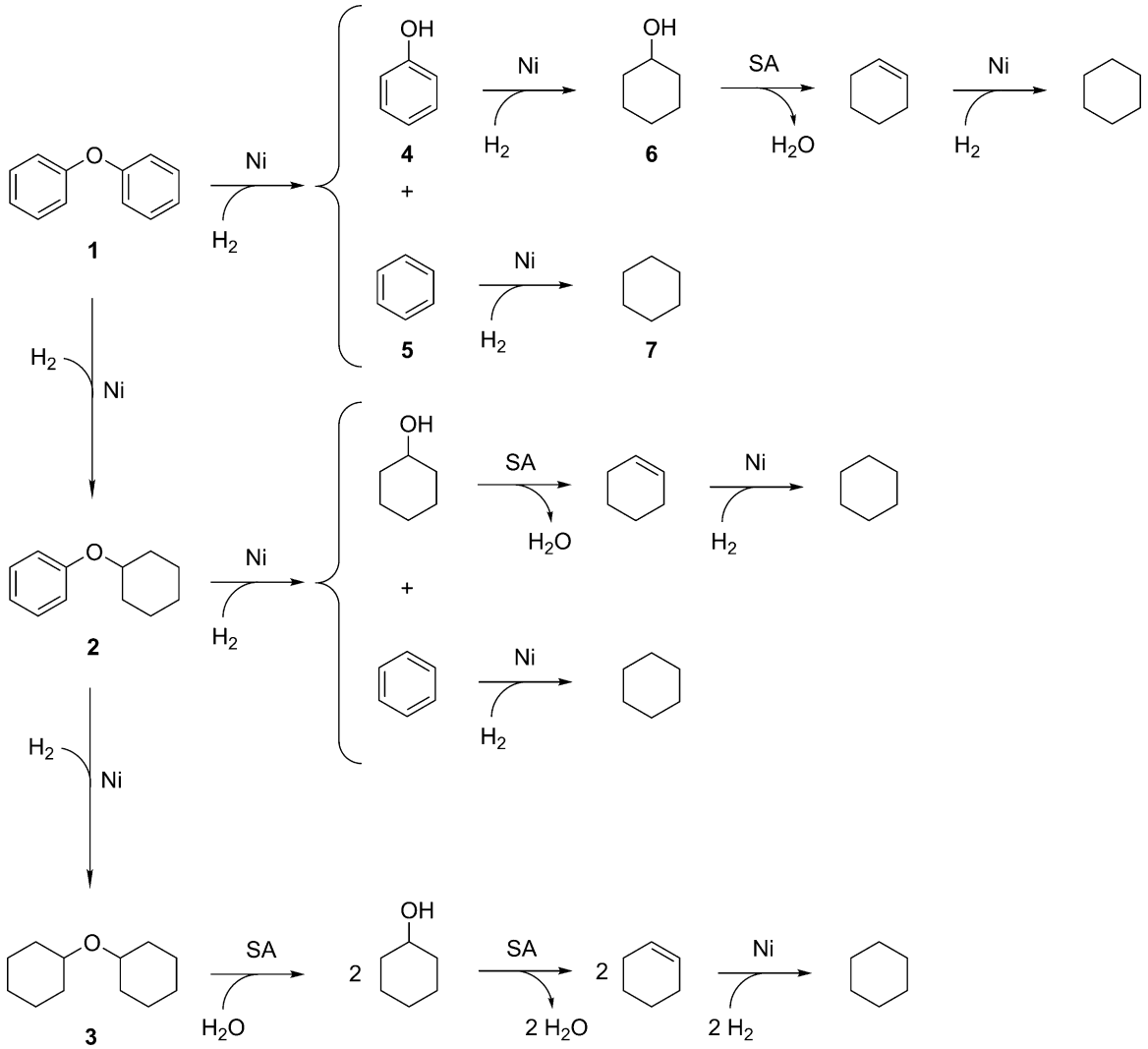

Scheme 1. Possible reaction channels involved in the conversion of diphenyl ether into cyclohexane. SA stands for solid acid.

H_2 (measured at room temperature) at 300 °C for 8 h. Under these conditions, an 84% conversion of Organosolv lignin was achieved, as determined by weight difference. To gain in-depth insight into the composition of the product mixture, the product mixture was analysed by using GC × GC–MS/FID.

Shown in Fig. 5 is GC × GC–MS image obtained from the product mixture. The amount of volatile compounds visible to the chromatographic analysis was estimated at approximately 45% (with an injector temperature of 300 °C). Remarkably, Organosolv lignin was almost fully converted into saturated hydrocarbons. Semiquantification by GC × GC–FID shows that more than 99% detected products are cycloalkanes, with only less than 1% cyclic alcohols remained as byproducts (retention time shorter than 9 min and not shown in Fig. 5). This result demonstrates that Ni/Al-SBA-15 can successfully catalyze the conversion of lignin into saturated alkanes through a one-pot process. Moreover, the current results starkly contrast to those reported by Toledano et al. [46,47] for conversion of lignin under microwave irradiation with hydrogen-donating solvents in the presence of Ni/Al-SBA-15. Under those conditions, the saturation of the phenolic ring could not be achieved by the H-transfer process, and therefore, extensive deoxygenation of the stream, *via* concurrent dehydration and hydrogenation, could not be accomplished. As a result, that process produced a mixture of phenols *via* the depolymerisation of lignin.

4. Conclusion

In this report, we demonstrated that Ni/Al-SBA-15 is a highly active catalyst for the hydrodeoxygenation of aromatic streams. Remarkably, full conversion of diphenyl ether into cyclohexane, in the presence of Ni/Al-SBA-15, was achieved. Organosolv lignin was also successfully converted into a mixture of cycloalkanes. Clearly, such a mixture of products is highly interesting for the production of drop-in transportation fuel because of the ease of product fractionation by conventional refining processes [48]. In a broader perspective, the current results also point to the importance of Al-SBA-15, as an acidic support alternative to zeolites or other acidic materials, for the HDO of phenolic streams.

Acknowledgements

The funds for this research were provided by the Alexander von Humboldt Foundation (Sofja Kovalevskaja Award 2010). This work was performed as part of the Cluster of Excellence “Tailor-Made Fuels from Biomass” (DFG).

References

[1] L.R. Lynd, C.H. de Brito Cruz, Science 330 (2010) 1176.

Please cite this article in press as: X. Wang, R. Rinaldi, Bifunctional Ni catalysts for the one-pot conversion of Organosolv lignin into cycloalkanes, Catal. Today (2016), http://dx.doi.org/10.1016/j.cattod.2015.11.047

[2] L.A. Horta Nogueira, J.R. Moreira, U. Schuchardt, J. Goldemberg, Energy Policy 61 (2013) 595–598.
[3] U. Schuchardt, T.T. Franco, J.C.P. de Melo, L.A.B. Cortez, Biofuels Bioprod. Biorefin. 8 (2014) 151–154.
[4] X. Wang, R. Rinaldi, ChemSusChem 5 (2012) 1455–1466.
[5] J.M.R. Gallo, J.M.C. Bueno, U. Schuchardt, J. Braz. Chem. Soc. 25 (2014) 2229–2243.
[6] C.O. Tuck, E. Pérez, I.T. Horváth, R.A. Sheldon, M. Poliakoff, Science 337 (2012) 695–699.
[7] A.J. Ragauskas, G.T. Beckham, M.J. Biddy, R. Chandra, F. Chen, M.F. Davis, B.H. Davison, R.A. Dixon, P. Gilna, M. Keller, P. Langan, A.K. Naskar, J.N. Saddler, T.J. Tschaplinski, G.A. Tuskan, C.E. Wyman, Science 344 (2014).
[8] R. Rinaldi, F. Schüth, Energy Environ. Sci. 2 (2009) 610–626.
[9] P.Y. Bi, J.C. Wang, Y.J. Zhang, P.W. Jiang, X.P. Wu, J.X. Liu, H. Xue, T.J. Wang, Q.X. Li, Bioresour. Technol. 183 (2015) 10–17.
[10] D.D. Laskar, B. Yang, H. Wang, J. Lee, Biofuels Bioprod. Biorefin. 7 (2013) 602–626.
[11] B. Joffres, D. Laurenti, N. Charon, A. Daudin, A. Quignard, C. Geantet, Oil Gas Sci. Technol. 68 (2013) 753–763.
[12] E. Dorrestijn, L.J.J. Laarhoven, I.W.C.E. Arends, P. Mulder, J. Anal. Appl. Pyrol. 54 (2000) 153–192.
[13] M. Kleinert, J.R. Gasson, T. Barth, J. Anal. Appl. Pyrol. 85 (2009) 108–117.
[14] P. Ferrini, R. Rinaldi, Angew. Chem. Int. Ed. 53 (2014) 8634–8639.
[15] S. Van den Bosch, W. Schutyser, R. Vanholme, T. Driessen, S.-F. Koelewijn, T. Renders, B. De Meester, W.J.J. Huijgen, W. Dehaen, C.M. Courtin, B. Lagrain, W. Boerjan, B. Sels, Energy Environ. Sci. 8 (2015) 1748–1763.
[16] S. Van den Bosch, W. Schutyser, S.F. Koelewijn, T. Renders, C.M. Courtin, B.F. Sels, Chem. Commun. 51 (2015) 13158–13161.
[17] T. Parsell, S. Yohe, J. Degenstein, T. Jarrell, I. Klein, E. Gencer, B. Hewetson, M. Hurt, J.I. Kim, H. Choudhari, B. Saha, R. Meilan, N. Mosier, F. Ribeiro, W.N. Delgass, C. Chapple, H.I. Kenttämaa, R. Agrawal, M.H. Abu-Omar, Green Chem. 17 (2015) 1492–1499.
[18] P.J. Deuss, M. Scott, F. Tran, N.J. Westwood, J.G. de Vries, K. Barta, J. Am. Chem. Soc. 137 (2015) 7456–7467.
[19] X. Huang, T.I. Koranyi, M.D. Boot, E.J.M. Hensen, Green Chem. (2015).
[20] B. Güvenatam, O. Kurşun, E.H.J. Heeres, E.A. Pidko, E.J.M. Hensen, Catal. Today 233 (2014) 83–91.
[21] E.L. Kunkes, D.A. Simonetti, R.M. West, J.C. Serrano-Ruiz, C.A. Gärtner, J.A. Dumesic, Science 322 (2008) 417–421.
[22] H. Kobayashi, H. Ohta, A. Fukuoka, Chapter 3 noble-metal catalysts for conversion of lignocellulose under hydrogen pressure, in: R. Rinaldi (Ed.), Catalytic Hydrogenation for Biomass Valorization, The Royal Society of Chemistry, 2015, pp. 52–73.
[23] C. Xu, R.A.D. Arancon, J. Labidi, R. Luque, Chem. Soc. Rev. 43 (2014) 7485–7500.
[24] P.M. Mortensen, J.D. Grunwaldt, P.A. Jensen, A.D. Jensen, ACS Catal. 3 (2013) 1774–1785.
[25] M. Stocker, Angew. Chem. Int. Ed. 47 (2008) 9200–9211.
[26] D.M. Alonso, S.G. Wettstein, J.A. Dumesic, Chem. Soc. Rev. 41 (2012) 8075–8098.
[27] M. Saidi, F. Samimi, D. Karimipourfard, T. Nimmanwudipong, B.C. Gates, M.R. Rahimpour, Energy Environ. Sci. 7 (2014) 103–129.
[28] C. Zhao, J. Lercher, Angew. Chem. 124 (2012) 6037–6042.
[29] C. Zhao, Y. Kou, A.A. Lemonidou, X. Li, J.A. Lercher, Chem. Commun. 46 (2010) 412–414.
[30] C. Zhao, Y. Kou, A. Lemonidou, X. Li, J. Lercher, Angew. Chem. 121 (2009) 4047–4050.
[31] P.M. Mortensen, J.D. Grunwaldt, P.A. Jensen, K.G. Knudsen, A.D. Jensen, Appl. Catal. A Gen. 407 (2011) 1–19.
[32] Dongyuan Zhao, Jianglin Feng, Qisheng Huo, Nicholas Melosh, Glenn H. Fredrickson, Bradley F. Chmelka, G.D. Stucky, Science 279 (1998) 548–552.
[33] Y. Yue, A. Gédéon, J.-L. Bonardet, N. Melosh, J.-B. D'Espinosea, J. Fraissarda, Chem. Commun. (1999) 1967–1968.
[34] Y. Li, W. Zhang, L. Zhang, Q. Yang, Z. Wei, Z. Feng, C. Li, J. Phys. Chem. B 108 (2004) 9739–9744.
[35] J.M.R. Gallo, C. Bisio, G. Gatti, L. Marchese, H.O. Pastore, Langmuir 26 (2010) 5791–5800.
[36] F. Su, J. Zeng, X. Bao, Y. Yu, J.Y. Lee, X.S. Zhao, Chem. Mater. 17 (2005) 3960–3967.
[37] J. Huang, S.-R. Wang, S.-H. Wu, J. Disper. Sci. Technol. 31 (2010) 1469–1473.
[38] R. Rinaldi, U. Schuchardt, J. Catal. 227 (2004) 109–116.
[39] A.V. Neimark, K.S.W. Sing, M. Thommes, Surface area and porosity, in: G. Ertl, H. Knözinger, F. Schüth, J. Weitkamp (Eds.), Handbook of Heterogeneous Catalysis, John Wiley & Sons, Inc., 2016, pp. 728–729.
[40] J. He, C. Zhao, J.A. Lercher, J. Am. Chem. Soc. 134 (2012) 20768–20775.
[41] J. He, L. Lu, C. Zhao, D. Mei, J.A. Lercher, J. Catal. 311 (2014) 41–51.
[42] J. He, C. Zhao, D. Mei, J.A. Lercher, J. Catal. 309 (2014) 280–290.
[43] K. Tanabe, W.F. Hölderich, Appl. Catal. A Gen. 181 (1999) 399–434.
[44] C. Zhao, Y. Kou, A.A. Lemonidou, X. Li, J.A. Lercher, Angew. Chem. Int. Ed. 48 (2009) 3987–3990.
[45] C. Zhao, Y. Kou, A.A. Lemonidou, X. Li, J.A. Lercher, Chem. Commun. 46 (2010) 412.
[46] A. Toledano, L. Serrano, J. Labidi, A. Pineda, A.M. Balu, R. Luque, ChemCatChem 5 (2013) 977–985.
[47] A. Toledano, L. Serrano, A. Pineda, A.A. Romero, R. Luque, J. Labidi, Appl. Catal. B Environ. 145 (2014) 43–55.
[48] X. Wang, R. Rinaldi, Angew. Chem. Int. Ed. 52 (2013) 11499–11503.

Please cite this article in press as: X. Wang, R. Rinaldi, Bifunctional Ni catalysts for the one-pot conversion of Organosolv lignin into cycloalkanes, Catal. Today (2016), http://dx.doi.org/10.1016/j.cattod.2015.11.047